Muscle Segment Homeobox Genes Direct Embryonic Diapause by Limiting Inflammation in the Uterus

Citation	Cha, J., Burnum-Johnson, K. E., Bartos, A., Li, Y., Baker, E. S., Tilton, S. C., ... & Dey, S. K. (2015). Muscle segment homeobox genes direct embryonic diapause by limiting inflammation in the uterus. Journal of Biological Chemistry, 290(24), 15337-15349. doi:10.1074/jbc.M115.655001
DOI	10.1074/jbc.M115.655001
Publisher	American Society for Biochemistry and Molecular Biology
Version	Version of Record
Terms of Use	http://cdss.library.oregonstate.edu/sa-termsofuse

THE JOURNAL OF BIOLOGICAL CHEMISTRY VOL. 290, NO. 24, pp. 15337–15349, June 12, 2015

Muscle Segment Homeobox Genes Direct Embryonic Diapause by Limiting Inflammation in the Uterus*[S]

Received for publication, April 7, 2015, and in revised form, April 21, 2015 Published, JBC Papers in Press, April 30, 2015, DOI 10.1074/jbc.M115.655001

Jeeyeon Cha[‡1], Kristin E. Burnum-Johnson[§1], Amanda Bartos[‡], Yingju Li[‡], Erin S. Baker[§], Susan C. Tilton[§¶], Bobbie-Jo M. Webb-Robertson[§], Paul D. Piehowski[‡], Matthew E. Monroe[§], Anil G. Jegga[‖], Shigeo Murata[**], Yasushi Hirota[‡‡], and Sudhansu K. Dey[‡2]

From the [‡]Division of Reproductive Sciences and [‖]Division of Biomedical Informatics, Cincinnati Children's Hospital Medical Center, Cincinnati, Ohio 45229-3039, the [§]Biological Sciences Division, Pacific Northwest National Laboratory, Richland, Washington 99354, the [¶]Environmental and Molecular Toxicology, Oregon State University, Corvallis, Oregon 97331, the [**]Laboratory of Protein Metabolism, Graduate School of Pharmaceutical Sciences, University of Tokyo, 7-3-1 Hongo, Bunkyo-ku, Tokyo 113-0033 Japan, and the [‡‡]Department of Obstetrics and Gynecology, Graduate School of Medicine, University of Tokyo, 7-3-1 Hongo, Bunkyo-ku, Tokyo 113-8655 Japan

Background: Embryonic diapause is a reproductive strategy that confers blastocyst dormancy and uterine quiescence without implantation until conditions become favorable.
Results: Mice devoid of uterine muscle segment homeobox genes (*Msx*) show heightened inflammatory signature with failure of diapause.
Conclusion: Msx coordinates various pathways limiting inflammation in the uterus for diapause.
Significance: This study identifies a previously unrecognized role of Msx in this unique phenomenon.

Embryonic diapause is a reproductive strategy widespread in the animal kingdom. This phenomenon is defined by a temporary arrest in blastocyst growth and metabolic activity within a quiescent uterus without implantation until the environmental and maternal milieu become favorable for pregnancy to progress. We found that uterine *Msx* expression persists during diapause across species; their inactivation in the mouse uterus results in termination of diapause with the development of implantation-like responses ("pseudoimplantation") that ultimately succumbed to resorption. To understand the cause of this failure, we compared proteome profiles between floxed and *Msx*-deleted uteri. In deleted uteri, several functional networks, including transcription/translation, ubiquitin-proteasome, inflammation, and endoplasmic reticulum stress, were dysregulated. Computational modeling predicted intersection of these pathways on an enhanced inflammatory signature. Further studies showed that this signature was reflected in increased phosphorylated IκB levels and nuclear NFκB in deleted uteri. This was associated with enhanced proteasome activity and endoplasmic reticulum stress. Interestingly, treatment with anti-inflammatory glucocorticoid (dexamethasone) reduced the inflammatory signature with improvement of the diapause phenotype. These findings highlight an unexpected role of uterine Msx in limiting aberrant inflammatory responses to maintain embryonic diapause.

Implantation is a complex process orchestrated by reciprocal interactions between the embryo and uterus. The orderly execution of this process is critical for pregnancy success. Implantation is one of the earliest encounters between the mother and conceptus, and it culminates from embryo development to the blastocyst stage synchronized with the acquisition of uterine receptivity for implantation. Any aberration in the implantation process can lead to pregnancy failure soon thereafter or can be propagated as adverse ripple effects through the remainder of pregnancy, resulting in compromised pregnancy outcome (1). Thus, the quality of implantation can dictate the course and outcome of pregnancy.

Implantation occurs within a defined time frame (window of implantation) in most eutherian mammals for appropriate synchrony of uterine readiness and embryo maturation to the blastocyst state. In all eutherian species studied to date, the uterus achieves this transient window of receptivity; in mice, this state lasts ~24 h and spontaneously transitions to a state refractory to implantation (2, 3). However, in many mammals, implantation can temporally disengage from parturition via embryonic diapause (delayed implantation), an evolutionarily conserved, natural pause in pregnancy prior to implantation. This phenomenon is defined by the temporary arrest of growth and metabolic activity of the embryo at the blastocyst stage in synchrony with uterine quiescence. This suspended state of pregnancy prevents blastocyst activation and implantation

* This work was supported in part by National Institutes of Health Grants R01ES022190, U01CA184783-01, R01HD068524, and P01CA77839. This work was also supported in part by the Laboratory Directed Research and Development Program at the Pacific Northwest National Laboratory (operated by Battelle for the Department of Energy under Contract DE-AC05–76RL01830), a Grant-in-Aid for Scientific Research from the Japan Society for the Promotion of Science; grants from the Astellas Foundation for Research on Metabolic Disorders, the Cell Science Research Foundation, the Tokyo Biochemical Research Foundation, and the Nakatomi Foundation (to Y. H.); grants the March of Dimes (to S. K. D.); and National Research Service Award Fellowship F30AG040858 of the University of Cincinnati Medical Scientist Training Program (to J. C.).
[S] This article contains supplemental Data Set S1.
[1] These authors contributed equally to this work.
[2] To whom correspondence should be addressed: Div. of Reproductive Sciences, Cincinnati Children's Hospital Medical Center, Cincinnati, OH 45229-3039. Tel.: 513-803-1158; Fax: 513-803-2090; E-mail: sk.dey@cchmc.org.

until environmental and maternal conditions are favorable for the survival and well-being of the mother and offspring.

Embryonic diapause has been identified in more than 100 species across seven orders and can last for days to months depending on the species (4, 5). Under favorable conditions, the uterus attains receptivity and the blastocyst is activated for implantation. Normally, delayed implantation can be induced during lactation after postpartum mating (facultative delay) or can occur in every gestation of a species (obligatory) influenced by photoperiod length and melatonin secretion.

Normally, delayed implantation in mice occurs naturally during lactation because of ovarian estrogen deficiency resulting from suckling stimulus; this stimulus increases prolactin release from the pituitary, decreasing ovarian estrogen secretion. Upon removal of sucking pups or estrogen administration, blastocyst activation occurs with initiation of implantation, resulting in successful pregnancy. Delayed implantation can also be induced by ovariectomizing pregnant mice on the morning of day 4 before preimplantation ovarian estrogen secretion. This condition can be maintained for days to weeks by providing daily progesterone (P_4)[3] in the absence of estrogen. With exposure to a small dose of estrogen in P_4-primed uteri of ovariectomized mice, blastocysts undergo activation with the initiation of implantation. With continued steroid treatment successful pregnancy occurs with delivery of pups. Irrespective of the type of delay, embryonic diapause is under maternal endocrine regulation in all species studied to date (4). However, the molecular mechanism by which these processes are regulated is not clearly understood (4–8).

We recently found that muscle segment homeobox genes (*Msx1* and *Msx2*), members of an ancient, evolutionarily conserved homeobox gene family, show persistent expression in mouse uteri during physiological or experimentally induced delayed implantation, suggesting that uterine *Msx* genes are critical for the initiation and maintenance of embryonic diapause (7). Indeed, mice with conditional uterine deletion of *Msx* genes (*Msx1/Msx2*$^{d/d}$) fail to undergo true delay. This is evident from poor blastocyst survival and often inappropriate manifestation of implantation-like responses ("pseudoimplantation") at the site of the blastocyst, which are not sustained and ultimately undergo resorption in *Msx1/Msx2*$^{d/d}$ mice (7). These findings suggested that Msx factors play a major role in the uterus to transiently confer uterine quiescence and blastocyst dormancy. We also observed persistent uterine expression of *Msx1* or *Msx2* in two other distantly related mammalian orders during diapause: Carnivora (American mink) and Diprotodontia (Australian tammar wallaby) (7). Taken together, these results suggest the presence of an evolutionarily conserved reproductive strategy across diverse mammalian species via uterine Msx (7).

To explore the mechanism by which Msx transcription factors regulate quiescence and maintain a uterine environment conducive to embryo survival, we performed proteomics analyses of littermate floxed (*Msx1/Msx2*$^{f/f}$) and *Msx1/Msx2*$^{d/d}$ mice under delayed implanting conditions experimentally induced by ovariectomy and P_4 treatment (6–8). These analyses identified several classes of signaling pathways enriched in transcription, translation, chromatin remodeling, inflammation, proteasome activity, ubiquitination, chaperone-mediated protein folding, oxidative, and ER stress responses in *Msx1/Msx2*$^{d/d}$ uteri. These findings were reflected in higher uterine levels of proteasome subunits, polyubiquitinated proteins, and ER stress consistent with proteotoxic stress/burden. Computational modeling predicted that these diverse pathways intersected on an enhanced inflammatory signature in *Msx1/Msx2*$^{d/d}$ uteri. These findings, coupled with our observations of failure of embryonic diapause with formation of pseudoimplantation sites in *Msx1/Msx2*$^{d/d}$ uteri, increased the signature of inflammation reflected in higher phosphorylated IκB (pIκB, nuclear factor of κ light polypeptide gene enhancer in B-cells inhibitor) levels and nuclear NFκB (nuclear factor κ-light-chain-enhancer of activated B cells) expression, and evidence of proteotoxic stress, are consistent with reported interactions between heightened proteasome activity with inflammation (9, 10). Aggravation of proteotoxicity with bortezomib resulted in an increased rate of pseudoimplantation in *Msx1/Msx2*$^{d/d}$ uteri, whereas inhibition of inflammatory response by dexamethasone substantially reduced the incidence and size of pseudoimplantation sites. In conclusion, this study identifies an unexpected role for *Msx* genes in limiting uterine stress-mediated inflammatory responses during embryonic diapause.

Experimental Procedures

Mice—Mice with uterine deletion of *Msx1* and *Msx2* (*Msx1/Msx2*$^{loxP/loxP}$ *Pgr*$^{Cre/+}$ = *Msx1/Msx2*$^{d/d}$) and control littermates (*Msx1/Msx2*$^{loxP/loxP}$ *Pgr*$^{+/+}$ = *Msx1/Msx2*$^{f/f}$) were generated as previously described (11). All protocols for the present study were reviewed and approved by the Cincinnati Children's Research Foundation Institutional Animal Care and Use Committee in accordance with National Institutes of Health guidelines. Adult *Msx1/Msx2*$^{f/f}$ and *Msx1/Msx2*$^{d/d}$ female mice were mated with fertile males to induce pregnancy (day 1 = vaginal plug).

Experimental Delay—To induce delayed implantation, plug-positive mice were ovariectomized on the morning of day 4 (0800–0900 h) and subcutaneously given P_4 in sesame oil daily (2 mg/100 μl/dose) on days 5–7 or 5–9 for tissue collection on day 8 or 10, respectively (7). For mass spectrometry analysis, uteri were flash-frozen and stored at −80 °C after gently flushing the horns with cold PBS containing protease and phosphatase inhibitors (Sigma) to recover embryos and to confirm pregnancy.

Pharmacological Treatments—The proteasome inhibitor bortezomib (0.2 mg/kg of body weight/day) was suspended in vehicle (5% v/v PEG400 and 5% v/v Tween 80 dissolved in water) and was given as a single oral gavage on days 5, 7, and 9 of pregnancy. A selective Cox2 inhibitor celecoxib (10 mg/kg of body weight/day) was suspended in vehicle (0.5% w/v methylcellulose and 0.1% v/v polysorbate 80 dissolved in water) and was given as a single oral gavage on days 5, 7, and 9 of pregnancy. Dexamethasone (20 μg/100 μl/dose) was injected subcutaneously on days 5–9 of pregnancy. Respective control groups received vehicle alone.

[3] The abbreviations used are: P_4, progesterone; pIκB, phosphorylated IκB; IMS, ion mobility spectrometry.

Mass Spectrometry Sample Preparation—Mass spectrometry was performed in the Environmental Molecular Sciences Laboratory, a U.S. Department of Energy Office of Biological and Environmental Research. Frozen tissue samples were plunged in LN_2 and immediately pulverized using a cryoPREP impactor (Covaris, Inc). Proteins were extracted with 500 μl of 8 M urea and 10 mM DTT in 100 mM ammonium bicarbonate at 37 °C for 1 h. Samples were centrifuged at 15,000 rpm to collect the supernatant. Protein extract (125 μg) was digested with sequencing grade trypsin (Promega) overnight with 1:50 enzyme: substrate ratio. The resulting peptides were desalted by C18 SPE (Supelco) and rehydrated in mobile phase A. Peptide concentration was measured by BCA assay (Thermo Scientific) and normalized to 0.5 μg/μl for LC-MS analysis.

LC-MS/MS and LC-MS Analyses—Analysis of the digested peptide mixtures from uterine tissues was performed on both a Thermo Fisher Scientific LTQ Orbitrap Velos mass spectrometer (San Jose, CA) operated in tandem MS (MS/MS) mode and an instrument built in-house that couples a 1-m ion mobility separation (12, 13) with an Agilent 6224 TOF MS that was upgraded to have a 1.5-meter flight tube for resolution of ~25,000. Two different LC systems were used for this analysis. The same fully automated two-column HPLC system built in-house (14) equipped with packed capillary columns was used for both instruments with mobile phase A consisting of 0.1% (v/v) formic acid in water and B comprised of 0.1% (v/v) formic acid in acetonitrile. A 100-min LC separation was performed on the Velos MS (using 60-cm-long columns having an outer diameter of 360 μm, an inner diameter of 75 μm, and 3-μm C_{18} packing material), whereas only a 60-min gradient with shorter columns (30-cm-long columns with the same dimensions and packing) was used with the ion mobility-MS (IMS-MS) because the additional IMS separation helps address detector suppression. Both gradients were linear increasing mobile phase B from 0 to 60% until the final 2 min of the run when B was purged at 95%. Each sample (5 μl) was injected for both analyses, and the HPLC was operated under a constant flow rate of 0.4 μl/min for the 100-min gradient and 1 μl/min for the 60-min gradient. The Velos MS data were collected from 400–2000 m/z at a resolution of 60,000 (automatic gain control target: 1×10^6) followed by data-dependent ion trap MS/MS spectra (automatic gain control target: 1×10^4) of the 12 most abundant ions using a collision energy setting of 35%. A dynamic exclusion time of 60 s was used to discriminate against previously analyzed ions. IMS-TOF MS data were collected from 100–3200 m/z.

Proteomics Data Processing and Statistical Analysis—Identification and quantification of the detected peptide peaks were performed using the accurate mass and time tag approach (15, 16). Peptide database generation utilized Velos tandem MS/MS data (17, 18). Because of the greater sensitivity and dynamic range of measurements (16), relative quantitation of peptide peaks utilized our IMS LC-MS data. Multiple bioinformatics tools developed in-house (19, 20) were used to process the IMS LC-MS data and correlate the resulting LC-MS features to our accurate mass and time tag database that contained IMS drift time, accurate mass, and LC separation elution time information for each peptide tag. Data processing of our 16 data sets (two uterine horns for each of four *Msx1/Msx2*$^{f/f}$ and four *Msx1/Msx2*$^{d/d}$ mice) included averaging peptide abundance data from the two uterine horns for each mouse. Further processing (21, 22) decreased our peptide value from 14,394 to 10,232 (*i.e.* peptides with inadequate data for statistics were removed). Normalization was performed using a rank invariant peptide subset that was in common between the two data sets (23). This rank invariant peptide subset was used for median centering of the data. Processing of the peptide data found 3,710 significant peptides at $p < 0.05$. These significant markers were used to generate signatures where each peptide increased, decreased, or had no statistical difference in the *Msx1/Msx2*$^{d/d}$ *versus Msx1/Msx2*$^{f/f}$ uteri. We then used the BP-Quant quantification (24) approach to estimate abundance at the protein level. There were a total of 1,019 significant proteins at $p < 0.05$. Of these significant proteins, 448 were identified by ≥2 peptides (supplemental Data Set S1, worksheets 1–4).

MetaCore Statistical Interactome—To identify major hubs or regulators of the significant proteins in *Msx1/Msx2*$^{d/d}$ uteri on day 8 of delayed implantation in comparison with control delayed uteri, the Statistical Interactome tool (MetaCore) was used to measure the interconnectedness of proteins in the experimental data set relative to all known interactions among all proteins measured in the study by hypergeometric distribution. Networks were constructed for experimental data and predicted hubs based on direct interactions from the Metacore knowledgebase and visualized in Cytoscape (25) (supplemental Data Set S1, worksheets 8 and 9).

Immunohistochemistry—Immunostaining was performed in formalin-fixed paraffin-embedded sections using antibodies to pIκB (rabbit, Cell Signaling, 9246), Rpn13 (rat, laboratory-generated), and Cox2 (rabbit, lab generated) as previously described (26).

Immunofluorescence—Frozen sections of *Msx1/Msx2*$^{d/d}$ uteri and control uteri were taken from snap frozen tissues at 12-μm thickness. Immunofluorescence was performed using NFκB (rabbit, sc-372), GRP78/Bip (goat, sc-1050), CD45 (rat, BioLegend, 103102), and F4/80 (mouse, Serotec, MCA497RT) antibodies after cold methanol or paraformaldehyde fixation. Cy3-conjugated donkey antibodies (Jackson ImmunoResearch Laboratories) were used for secondary antibodies. Nuclear staining was performed with Hoescht 33342. Immunofluorescence was visualized with confocal microscopy (Nikon Eclipse TE2000).

Immunoblotting—Protein extraction and Western blotting were performed as previously described (14). Antibodies to phosphorylated IκB (mouse, Cell Signaling Technology, 9246), total IκB (rabbit, Cell Signaling Technology, 9242), 20S proteasome α-1, 2, 3, 5, 6, 7 subunits (mouse, Enzo, MCP231), α6 (rabbit, laboratory-generated), Rpt6 (mouse, laboratory-generated), Rpn8 (rabbit, laboratory-generated), HSPA5/Bip (goat, sc-1050), phosphorylated eIF2α (rabbit, Cell Signaling, 3597S), total eIF2α (rabbit, sc-11386), ubiquitin lysine 48 (rabbit, Millipore, 05-1307), and ubiquitin lysine 63 (rabbit, Millipore, 05-1308) were used as previously described (27). Actin (goat, sc-1615) served as a loading control.

Statistical Analysis—Statistical analyses of proteomic data were performed using two-tailed Student's t test for quantita-

tive comparisons and a g-test for qualitative comparisons as appropriate (22). Values of $p < 0.05$ were considered statistically significant.

Results

Msx1/Msx2$^{d/d}$ Uteri Fail to Undergo True Delay under Experimental Conditions—In mice, delayed implantation induced experimentally by ovariectomy on the morning of day 4 prior to preimplantation estrogen secretion can be maintained for days to weeks with continued P_4 administration (Fig. 1*A*) (7). *Msx1/Msx2*$^{d/d}$ females showed reduced blastocyst recovery and often inappropriate manifestation of some implantation-like responses ("pseudoimplantation") at the site of the blastocyst predominantly by day 10 of delayed implantation (6 days of dormancy) in the absence of estrogen; these pseudoimplantation sites underwent resorption (Fig. 1, *B* and *C*). Blastocyst recovery showed unhealthy embryos with some cells adherent to the abembryonic pole. These pseudoimplantation sites showed signs of increased vascular permeability by blue dye assay (3, 29), albeit at different intensities, with swellings of variable sizes. In contrast, no such swellings or blue reaction was noted in littermate floxed females under similar conditions.

Msx1/Msx2$^{d/d}$ Uteri Show a Unique Proteome Signature under Delayed Conditions That Intersects on Inflammation—To identify molecular targets of Msx transcription factors, we compared proteomics profiles between *Msx1/Msx2*$^{f/f}$ and *Msx1/Msx2*$^{d/d}$ uteri on day 8 of delayed implantation (4 days of dormancy). Our analysis identified 448 proteins by ≥2 peptides ($p < 0.05$) (Fig. 2*A* and supplemental Data Set S1, worksheets 1–4) (24). We performed comparisons of enriched gene ontology and pathway designations within the up-regulated and down-regulated proteins using the programs ToppGene Suite (30) and ToppCluster (31) ($p < 0.05$ with FDR correction) and resolved the most significantly enriched gene ontology biological processes and pathways (supplemental Data Set S1, worksheets 5 and 6). Computational modeling was performed with networks containing select enriched terms to visualize relevant functional relationships using Cytoscape in a spring embedded layout function (25). We identified multiple interactions between pathways, particularly for inflammatory response, NFκB-mediated inflammation, kinases of NFκB inhibitor IκB (IKKβ and IKKε), ubiquitin-proteasome system, ER stress, chaperone-mediated protein folding, oxidative stress, and antioxidant activity (Fig. 2*B* and supplemental Data Set S1, worksheet 7).

To identify a common hub among all dysregulated pathways in the context of inflammation, we utilized the Statistical Interactome tool (MetaCore, Thomson Reuters, Philadelphia, PA). This tool allowed us to assess the interconnectedness of proteins in the experimental data set relative to all known interactions among all proteins measured in the study by hypergeometric distribution to delineate major hubs or regulators of significantly altered proteins in *Msx1/Msx2*$^{d/d}$ uteri (Fig. 3 and supplemental Data Set S1, worksheet 8). Networks were constructed for experimental data and predicted hubs based on direct interactions from the Metacore knowledgebase. Interestingly, significant hubs for the proteins altered in *Msx1/Msx2*$^{d/d}$ uteri under delayed conditions included NFκB subunits RelA/p65 and c-Rel, IKK-ε (IKKE), IKK-β (IKKB), SAM68, NF-X1, TGM2, and Fetuin-A (supplemental Data Set S1, worksheet 9), identifying enriched interconnectedness of the proteins within the data set for the NFκB signaling pathway and inflammation.

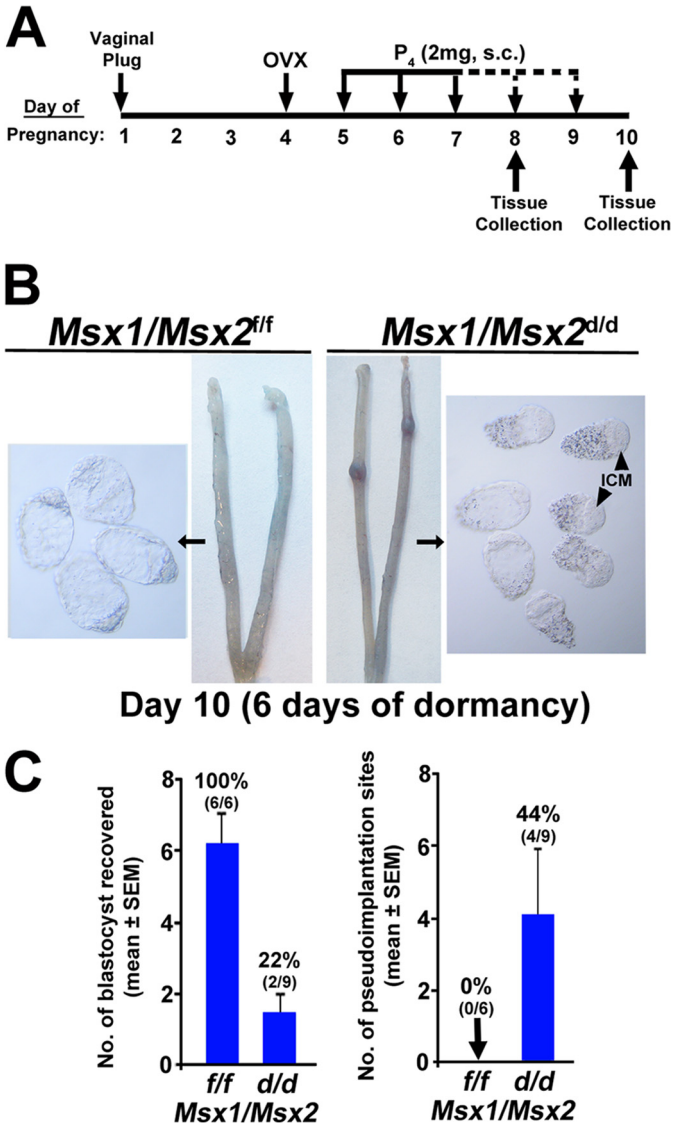

FIGURE 1. **Mice with uterine deletion of *Msx* genes fail to undergo true delay.** *A*, schematic protocol for experimentally inducing delayed implantation. On the morning of day 4 of pregnancy, plug-positive females were ovariectomized (*OVX*) and then administered P_4 daily (2 mg, subcutaneously) from day 5 until the day prior to tissue collection. *B*, littermate *Msx1/Msx2*$^{f/f}$ and *Msx1/Msx2*$^{d/d}$ females were injected with a blue dye prior to tissue collection. On day 10, a subset of P_4-treated, *Msx1/Msx2*$^{d/d}$ uteri showed small swellings (pseudoimplantation sites) of various sizes, some of which showed leakage of blue dye, at the sites of blastocysts. Blastocysts recovered from *Msx1/Msx2*$^{d/d}$ females showed signs of degeneration and poor morphological appearance, several of which showed some cells adherent to the abembryonic trophectoderm. *Arrowheads*, inner cell mass (*ICM*). *C*, blastocysts recovery (*left bar graph*) and incidence of pseudoimplantation (*right bar graph*) from ovariectomized, P_4-treated *Msx1/Msx2*$^{f/f}$ and *Msx1/Msx2*$^{d/d}$ females on day 10 (means ± S.E.). *Numbers* in *parentheses* indicate number of females that produced blastocysts or pseudoimplantation sites, respectively, with respect to the number of females examined.

Inflammatory Responses Are Up-regulated in Msx1/Msx2$^{d/d}$ Uteri under Delayed Conditions—Considering our phenotype of pseudoimplantation sites in *Msx1/Msx2*$^{d/d}$ uteri under

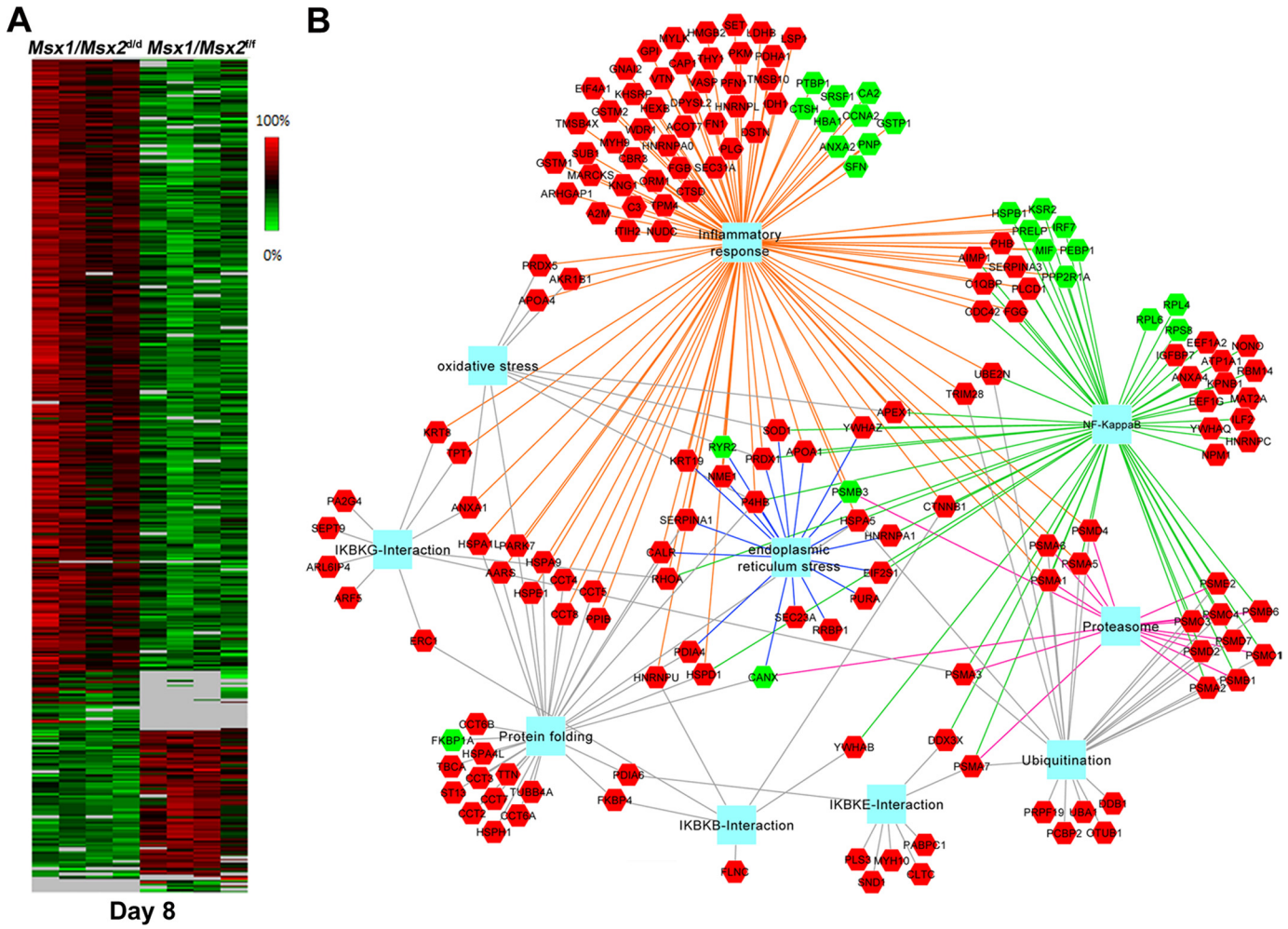

FIGURE 2. ***Msx1/Msx2*$^{d/d}$ uteri show unique proteomics signature under delayed conditions.** *A*, heat map depicting 448 significantly changing protein levels in *Msx1/Msx2*$^{d/d}$ uteri under delayed conditions. Relative protein intensities were measured by ion mobility mass spectrometry from eight mice under delayed implanting conditions ($n = 4$ each of genotype; $p < 0.05$). All proteins were identified by at least two peptides). *B*, a network representation of a subset of significant proteins in *Msx1/Msx2*$^{d/d}$ uteri (*red* and *green hexagons* represent up- and down-regulated proteins, respectively). Key enriched biological processes and pathways ($p < 0.05$ with FDR correction) are represented as *blue squares*, connected to associated proteins by *lines*. Connections between proteins and inflammation, NFκB, proteasome, and endoplasmic reticulum stress are highlighted as *orange*, *green*, *pink*, and *blue lines*, respectively. All other lines are represented in *gray*.

delayed conditions (7), we were intrigued by the changes in regulatory pathways of inflammation identified by our proteomics and computational analysis. We found up-regulation of several proteins involved in inflammation and acute inflammatory responses in *Msx1/Msx2*$^{d/d}$ uteri, such as α2-macroglobulin, LSP1 (lymphocyte-specific protein 1), KNG1 (kininogen), complement components (C1qbp and C3), Park 7 (Parkinson protein 7), IL enhancer binding factor 2, and importin β-subunit 1 (KPNB1) (supplemental Data Set S1, worksheets 4 – 6). Notably, we previously identified up-regulation of epithelial *C3* expression in *Msx1/Msx2*$^{d/d}$ uteri (11). In contrast, interferon regulatory factor 7y, monocyte inhibitory factor, and Ig chains were down-regulated (supplemental Data Set S1, worksheets 4 – 6).

To evaluate the status of NFκB-mediated inflammation, we examined the status of uterine levels of pIκB. Phosphorylation of IκB by IKK allows for ubiquitination and degradation of IκB, permitting NFκB dissociation and translocation to the nucleus. Indeed, Western blotting results showed enhanced IκB phosphorylation on day 8 in *Msx1/Msx2*$^{d/d}$ uteri (Fig. 4*A*). This was reflected in increased uterine immunolocalization of pIκB on days 8 and 10 along with increased nuclear NFκB localization on day 10, particularly in the epithelium and subepithelial stroma of *Msx1/Msx2*$^{d/d}$ uteri (Fig. 4, *B* and *C*). Notably, there were insignificant changes in the distribution of leukocytes and macrophages between floxed and *Msx1/Msx2*$^{d/d}$ uteri (Fig. 4*D*). Our previous study showed *Ptgs2* expression (encoding Cox2) in the luminal epithelium and subepithelial stroma at the pseudoimplantation sites of *Msx1/Msx2*$^{d/d}$ mice with embryos entrapped within the intact luminal epithelium (7). Here we show by immunohistochemistry that Cox2 is also expressed in the luminal epithelium of *Msx1/Msx2*$^{d/d}$ uteri away from the site of blastocyst on day 10 of pregnancy (day 6 of dormancy); no such expression was noted in floxed uteri under similar conditions (Fig. 4*E*). In addition, pseudoimplantation sites showed modest decidualization on day 10 in the absence of luminal epithelial breaching, suggesting that the embryo transmitted some signals through *Msx*-deleted luminal epithelium to the subepithelial stroma (Fig. 4*F*). However, these responses were unsustainable, leading to resorption (7). Taken together, these

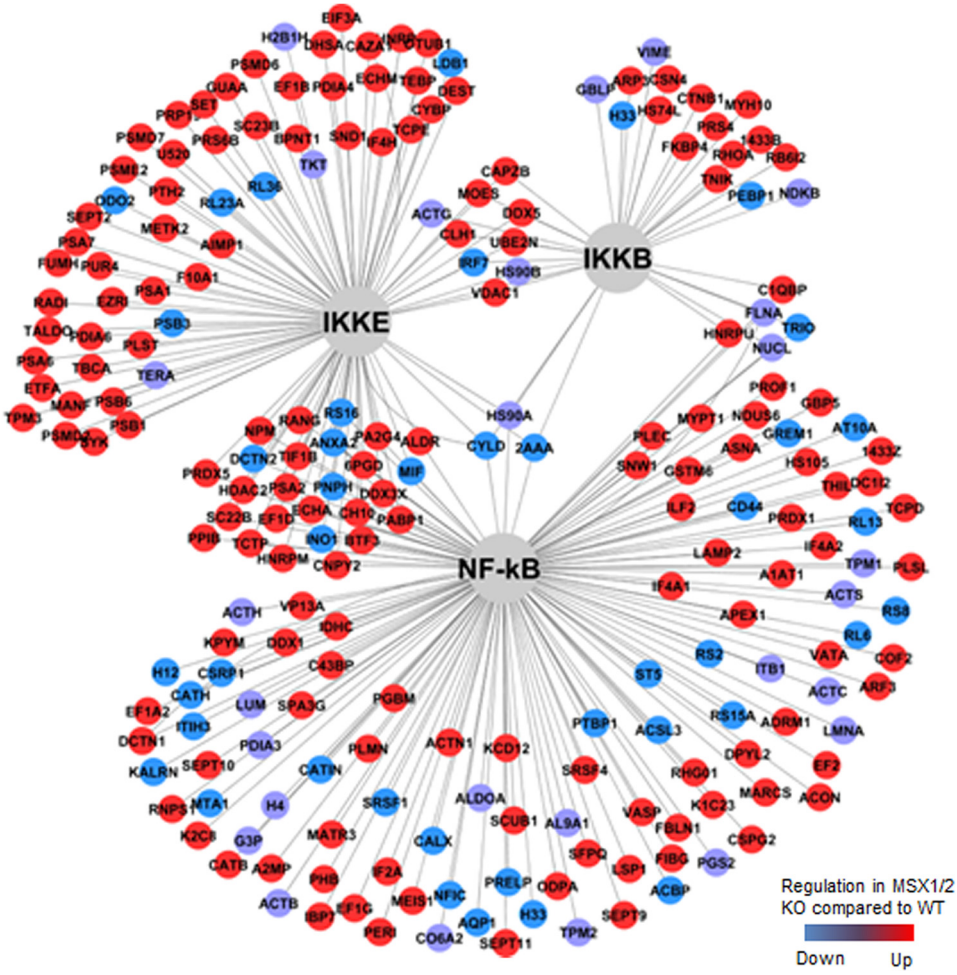

FIGURE 3. **MetaCore network analysis of proteins changed in *Msx1/Msx2*$^{d/d}$ mice showed increased connectivity with the inflammatory NFκB pathway.** *Red*, increased in *Msx1/Msx2*$^{d/d}$ mice compared with *Msx1/Msx2*$^{f/f}$ mice; *blue*, decreased in *Msx1/Msx2*$^{d/d}$ mice compared with *Msx1/Msx2*$^{f/f}$ mice; *purple*, significant trends in both directions.

results suggest that inflammatory responses seen in *Msx1/Msx2*$^{d/d}$ uteri under delayed conditions are mediated by increased NFκB signaling and are consistent with aberrant Cox2 expression, as observed in other systems (32–36).

The Ubiquitin-Proteasome System Is Enriched in Msx1/Msx2$^{d/d}$ *Uteri under Delayed Conditions*—We next asked what contributes to the enhanced inflammatory responses in *Msx1/Msx2*$^{d/d}$ uteri under delayed conditions. In addition to several proteins implicated in translation and secretory machinery, we found that numerous proteasome core and regulatory components were up-regulated in *Msx*-deleted uteri (supplemental Data Set S1, worksheets 4 – 6). The proteasome system encompasses a highly conserved and regulated network of proteins that normally degrade damaged and/or misfolded proteins to maintain protein homeostasis. They also participate in cell cycle regulation, protein turnover, gene expression, immune response, and responses to oxidative stresses (37–40). There is evidence that proteasome activity is correlated with heightened inflammation secondary to increased intracellular protein turnover and antigen processing (9, 10, 41). Furthermore, accumulation of misfolded proteins can lead to harmful effects collectively known as proteotoxicity (42).

The key enzyme responsible for mammalian proteolysis is the 26S proteasome, which is comprised of the barrel-shaped 20S core particle consisting of unique outer α- and inner β-subunits and two 19S regulatory particles. The 19S particle is further subdivided into a 9-subunit base that directly interacts with the α-ring of the 20S core particle and a 10-subunit lid. These components confer substrate specificity and other minor enzymatic activities for proteolysis. To confirm the up-regulation of proteasome components in *Msx1/Msx2*$^{d/d}$ uteri, we examined the α-subunits of the 20S core identified in our proteomics analysis by Western blotting and found their up-regulation along with increased levels of the specific core α-subunit 6 (α6), lid subunit Rpn8, and base subunit Rpt6 in *Msx1/Msx2*$^{d/d}$ uteri on day 10 (Fig. 5, *A* and *B*, and supplemental Data Set S1, worksheets 4 – 6).

The ubiquitin-proteasome system targets proteins for degradation by polyubiquitination (43). We next assessed whether our proteomics analysis showed dysregulation of ubiquitination pathway components in *Msx1/Msx2*$^{d/d}$ uteri. We found elevated protein levels of ubiquitin regulators (supplemental Data Set S1, worksheets 4 – 6). Ubiquitin chains can be formed by lysine linkages either via Lys-48 or Lys-63, and these linkages

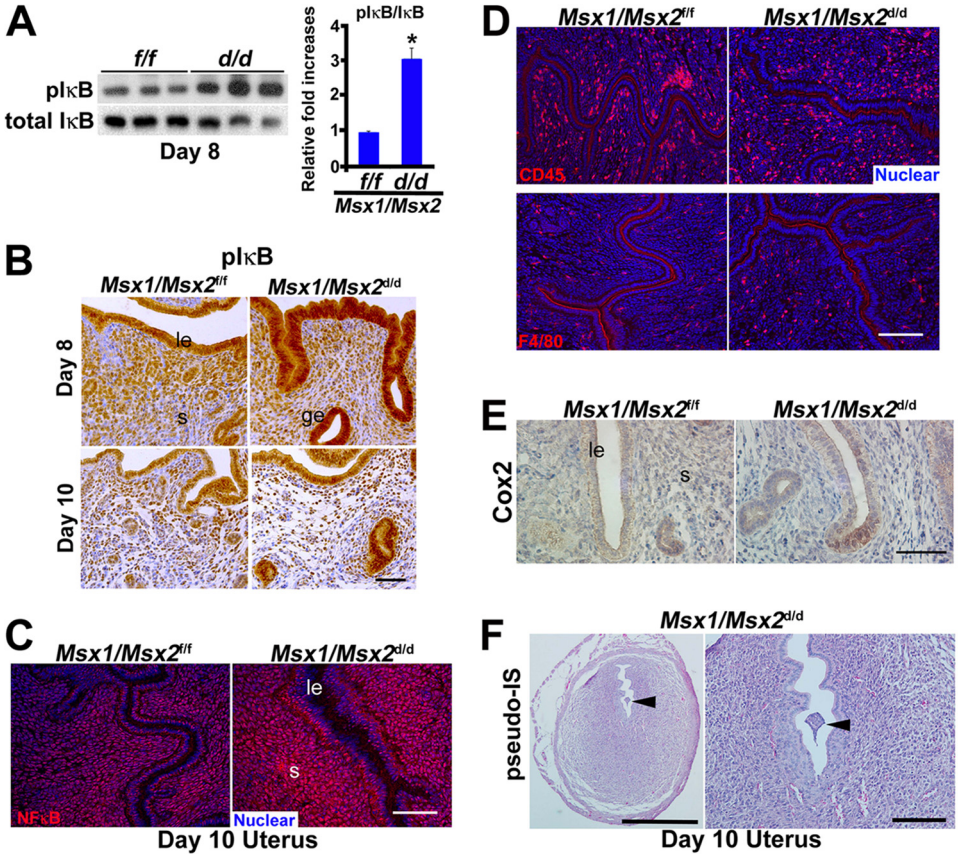

FIGURE 4. ***Msx1/Msx2*$^{d/d}$ uteri show enhanced uterine inflammation under delayed conditions.** *A*, Western blotting results showing increased levels of phosphorylated IκB (pIκB) in *Msx1/Msx2*$^{d/d}$ uteri under delayed conditions on day 8. *Bar diagram*, quantification of pIκB ($n = 3$ females/genotype, means ± S.E.; *, $p = 0.03$). *B*, immunohistochemistry for pIκB in *Msx1/Msx2*$^{f/f}$ and *Msx1/Msx2*$^{d/d}$ uteri under delayed conditions on days 8 and 10. *C*, immunofluorescence for NFκB in *Msx1/Msx2*$^{f/f}$ and *Msx1/Msx2*$^{d/d}$ uteri under delayed conditions on day 10. *Bar*, 100 μm. *D*, immunofluorescence for CD45 and F4/80 in *Msx1/Msx2*$^{f/f}$ and *Msx1/Msx2*$^{d/d}$ uteri under delayed conditions on day 10. *Bar*, 100 μm. *E*, immunohistochemistry of Cox2 in the luminal epithelium in *Msx1/Msx2*$^{f/f}$ and *Msx1/Msx2*$^{d/d}$ uteri on day 10. *F*, representative histological section of a pseudoimplantation site in *Msx1/Msx2*$^{d/d}$ uterus delayed conditions on day 10. The hematoxylin/eosin-stained section shows intact luminal epithelium and initiation of stromal decidualization. *Arrowhead*, embryo. *Bar*, 500 μm. *Lower power scale bar*, 500 μm; *higher power scale bar*, 100 μm. *le*, luminal epithelium; *ge*, glandular epithelium; *s*, stroma.

appear to be enhanced for either proteasome degradation or signaling, respectively (38). Interestingly, enhanced polyubiquitination via linker Lys-48 in *Msx1/Msx2*$^{d/d}$ uteri under delayed conditions was identified by Western blotting; Lys-63 linkages were undetectable (Fig. 5*B*). Furthermore, immunohistochemistry in *Msx1/Msx2*$^{d/d}$ uteri on day 10 showed higher levels of Rpn13/ADRM1, a proteasome regulatory subunit and ubiquitin receptor (Fig. 5*C*) (44). This expression was pronounced in the luminal and glandular epithelia, the site of *Msx* expression during delayed implantation in floxed uteri. Overall, these results suggest that *Msx1/Msx2*$^{d/d}$ uteri have enhanced proteasome expression and accumulation of ubiquitinated proteins targeted for proteasome degradation compared with *Msx1/Msx2*$^{f/f}$ uteri under similar experimental conditions.

Chaperone and Co-chaperone Proteins Are Up-regulated in the Msx1/Msx2$^{d/d}$ *Uterus under Delayed Conditions*—Molecular chaperones and co-chaperones are critical for distinguishing normal *versus* misfolded proteins; they facilitate correct folding or ubiquitin-mediated proteasomal degradation of aberrant proteins (45, 46). Accumulation of misfolded proteins can lead to proteotoxic stress and inflammation (47–49). Proteotoxicity in the cytosol can initiate the unfolded protein response, resulting in ER stress. This response results in decreased translation and increased heat shock protein response to help protein refolding or degradation (42). In this respect, heat shock proteins HSP10, HSP70, HSP105, HSPA5 (Bip), GRP75, chaperonin 60, T-complex protein 1 (TCP1, multiple subunits), and immunophilin FKBP4 (FKBP52) were all up-regulated in *Msx1/Msx2*$^{d/d}$ uteri (supplemental Data Set S1, worksheets 4–6). Interestingly, mice missing FKBP4 (FKBP52) show pregnancy failure because of diminished P_4 sensitivity, which is reversed by exogenous P_4 administration (50, 51). In addition, Bip is a marker of ER stress involved in the unfolded protein response and is also expressed in the mouse uterus (52, 53). We indeed found increased levels and expression of Bip at the apical surface of the epithelium and in interspersed subepithelial stromal cells in *Msx1/Msx2*$^{d/d}$ uteri (Figs. 5*D* and 6*A*), suggesting heightened ER stress.

Under normal conditions, Bip binds to the luminal domains of ER transmembrane proteins IRE1 (inositol requiring 1), PRK-like ER kinase (54), and ATF6 (activating transcription factor 6). During conditions of ER stress, Bip dissociates from these sensors for activation of the unfolded protein response to restore protein homeostasis (55). Our proteomics results had identified increased levels of eIF2α in *Msx1/Msx2*$^{d/d}$ uterus under delayed conditions. Phosphorylation of eIF2α is a surro-

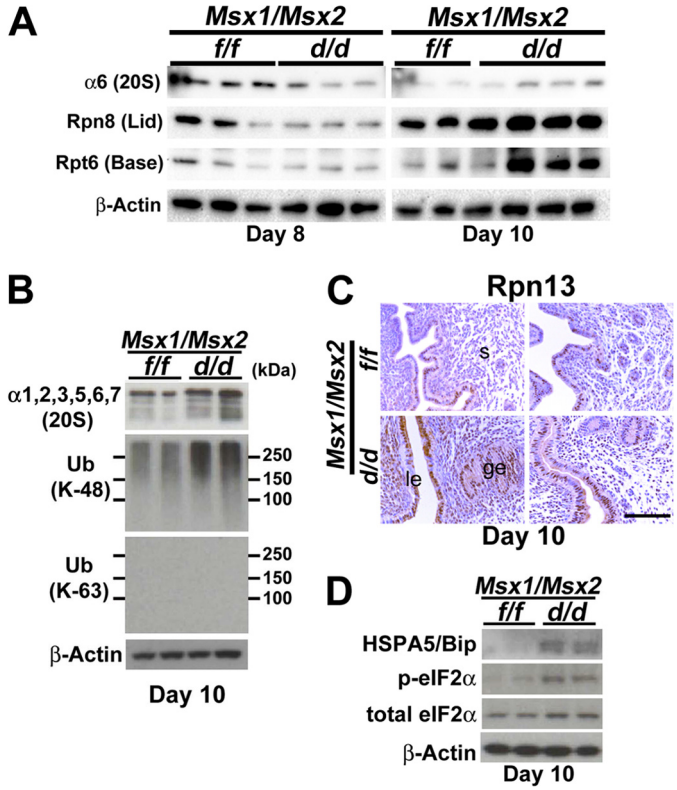

FIGURE 5. **Ubiquitin-proteasome pathway components are up-regulated in *Msx1/Msx2*$^{d/d}$ uteri under delayed conditions.** *A*, Western blotting results depicting increased levels of α6 subunit (20S core), Rpn8 (lid), and Rpt6 (base) components of the proteasome in *Msx1/Msx2*$^{d/d}$ uteri on days 8 and 10 under delayed conditions. *B*, Western blotting results showing increased levels of α-subunits of the 20S core proteasome and polyubiquitination of proteins via lysine 48 linkages, but not lysine 63 linkages in *Msx1/Msx2*$^{d/d}$ mice on day 10 under delayed conditions. *C*, immunohistochemistry results showing enhanced staining for ubiquitin receptor and proteasome regulatory component Rpn13 in *Msx1/Msx2*$^{d/d}$ uterine epithelium under delayed conditions. *le*, luminal epithelium; *ge*, glandular epithelium; *s*, stroma. *Bar*, 200 μm. *D*, Western blotting results showing increased levels of HSPA5 (Bip), p-eIF2α, and eIF2α in *Msx1/Msx2*$^{d/d}$ mice on day 10 under delayed conditions.

gate marker of PERK activation (56). We indeed found increased levels of phospho-eIF2α and total eIF2α, consistent with higher Bip expression in *Msx1/Msx2*$^{d/d}$ uterus (Fig. 5*D*).

Bortezomib Treatment Exacerbates ER Stress with Increased Incidence of Pseudoimplantation in Msx1/Msx2$^{d/d}$ *Females*—We initially speculated that proteasome function contributed to the inflammatory response seen in *Msx1/Msx2*$^{d/d}$ uteri and that inhibition of proteasome function may ameliorate inflammation and improve delayed implantation in *Msx1/Msx2*$^{d/d}$ uteri. Therefore, we treated *Msx1/Msx2*$^{d/d}$ females with an inhibitor of proteasome activity, bortezomib. To our surprise, we found that this inhibitor rather aggravated the incidence of pseudoimplantation sites in *Msx1/Msx2*$^{d/d}$ females under delayed conditions (100% with bortezomib treatment *versus* 44% without treatment) with further reduction in blastocyst recovery (Figs. 1*C* and 6*B*). Bortezomib had negligible effects on *Msx1/Msx2*$^{f/f}$ uteri under similar conditions (Fig. 6*B*), presumably because of sustained *Msx1* expression in the mouse uterus under normal delayed conditions (7). These results implicate that increased proteasome activity in the absence of *Msx* was to counteract the burden of unfolded/misfolded proteins caused by enhanced translation and ER stress. This is consistent with increased incidence of pseudoimplantation sites with bortezomib (57). Indeed, we found increased population of Bip-positive cells and higher Bip levels in bortezomib-treated *Msx1/Msx2*$^{d/d}$ uteri consistent with aggravated ER and proteotoxic stress (Fig. 7, *A–C*) (58). These results corroborate a report of the potential mechanism of action of bortezomib in cancer by increasing proteotoxic stress in susceptible, malignant cells toward apoptosis (42). Increases in pIκB levels and enhanced nuclear localization of NFκB were also observed in *Msx1/Msx2*$^{d/d}$ uterine samples after bortezomib treatment (Fig. 7, *A*, *B*, and *D*). These findings indicate that the up-regulation of proteasome subunits in these mice perhaps attempted to limit, rather than direct, the protein burden, unfolded protein response and inflammatory responses after *Msx* inactivation in the uterus but failed to suppress the inflammation.

Given these findings, we reasoned that inhibition of inflammation by an anti-inflammatory agent will attenuate the adverse phenotypes of *Msx1/Msx2*$^{d/d}$ uteri under delayed conditions. We first used a selective Cox inhibitor (celecoxib) in *Msx1/Msx2*$^{d/d}$ females under delayed conditions to improve embryonic diapause phenotype. We found modest improvement with a reduction in the incidence of pseudoimplantation site (Fig. 8*A*). We next used a prototypical anti-inflammatory steroid dexamethasone that has been shown to inhibit NFκB-mediated inflammation (34). Dexamethasone acts via glucocorticoid receptor in the rodent uterus to limit epithelial cell proliferation and estrogen-induced implantation (59, 60). Indeed, treatment with dexamethasone substantially reduced the incidence and size of pseudoimplantation sites in *Msx1/Msx2*$^{d/d}$ uteri with attenuated expression of nuclear NFκB, as well as levels of pIκB and proteasome subunits of 20S (Fig. 8, *A–D*). Dexamethasone also inhibited levels of eIF2α, p-eIF2α, and Bip (Fig. 8*C*).

Discussion

Msx genes are critical for uterine receptivity and implantation (11), and they have indispensable roles in the onset and maintenance of delayed implantation by conferring blastocyst dormancy and uterine quiescence (7). Wild-type uteri under delayed conditions show persistent *Msx1* expression and remain quiescent without any sign of implantation or endometrial vascular permeability at the site of blastocyst apposition (7, 11, 61). In contrast, mice with conditional uterine inactivation of *Msx1* and *Msx2* fail to undergo true delay and manifest unique phenotypes—continued cell proliferation in the blastocyst and formation of pseudoimplantation sites in the uterus at the site of the blastocyst without trophectoderm invasion through the luminal epithelium. Although implantation can be initiated in delayed implanting floxed mice if estrogen is given after P_4 priming, our observation of pseudoimplantation in *Msx1/Msx2*$^{d/d}$ uteri in the absence of estrogen suggests that a different mechanism is operative to terminate delayed implantation. Thus, although termination of diapause in the absence of *Msx* is not physiological and leads to resorption with pregnancy failure, termination of diapause in P_4-treated floxed mice after estrogen exposure is physiological and results in a live birth.

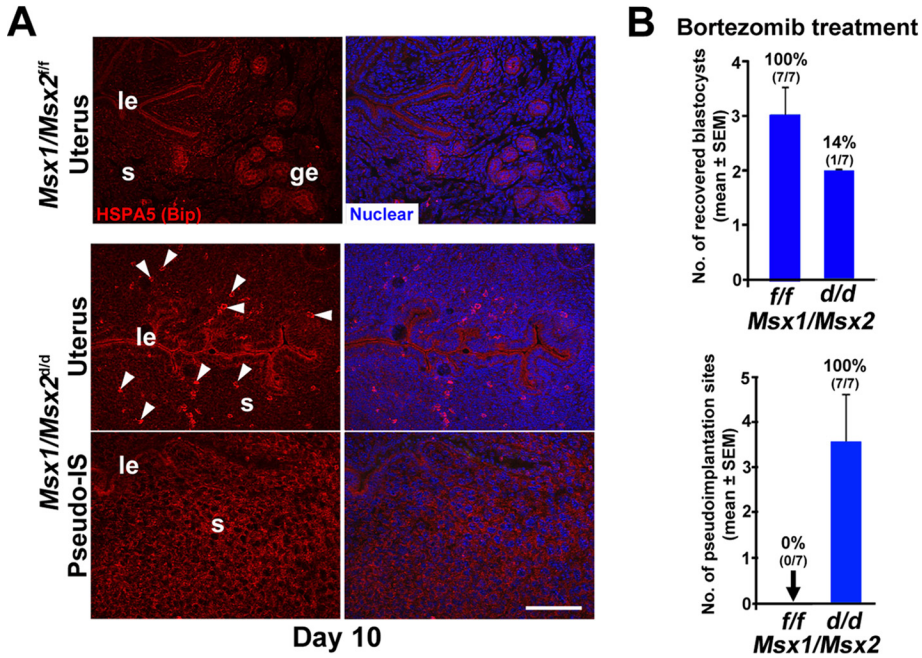

FIGURE 6. **ER stress is evident in *Msx1/Msx2*$^{d/d}$ uteri under delayed conditions and is aggravated by bortezomib treatment.** *A*, representative results of immunofluorescence showing apical epithelial expression of HSPA5/Bip in *Msx1/Msx2*$^{f/f}$ uteri, with increased intensity and dispersed Bip-positive stromal cells in *Msx1/Msx2*$^{d/d}$ uteri. Stromal Bip expression is widespread at the pseudoimplantation site (*Pseudo-IS*). *Arrowheads*, dispersed Bip-positive cells. *Bar*, 250 μm. *B*, blastocysts recovery (*top bar graph*) from *Msx1/Msx2*$^{d/d}$ after bortezomib treatment females was significantly lower with enhanced rate of pseudoimplantation sites (*bottom bar graph*) compared with floxed littermates on day 10 (means ± S.E.). *Numbers* in *parentheses* indicate number of females that produced blastocysts or pseudoimplantation sites, respectively, compared with the number of females assessed.

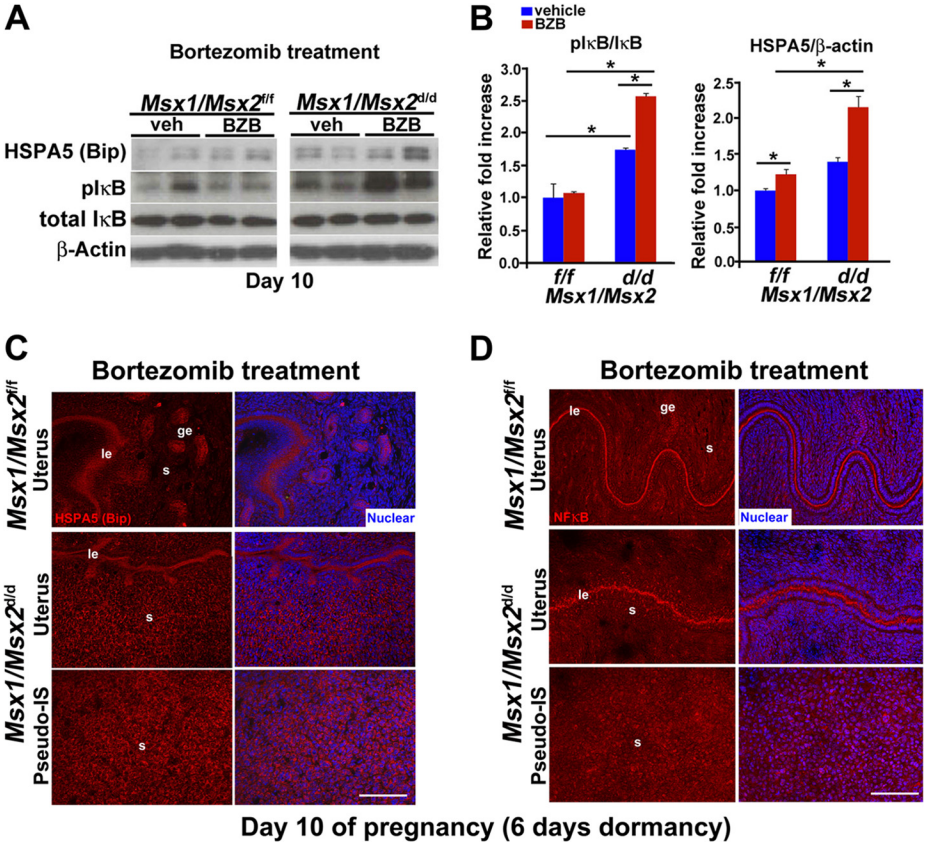

FIGURE 7. **Aggravation of ER stress and inflammation by bortezomib treatment in *Msx1/Msx2*$^{d/d}$ uteri under delayed conditions.** *A*, Western blotting results showing increased levels of Bip and pIκB in *Msx1/Msx2*$^{d/d}$ mice after bortezomib (*BZB*) treatment. *B*, quantification of Western blotting results (means ± S.E.; *, $p < 0.05$). *C*, immunofluorescence showing increased Bip expression in *Msx1/Msx2*$^{d/d}$ uterine sections and pseudoimplantation sites (*Pseudo-IS*) under delayed conditions compared with floxed littermates after bortezomib treatment. *D*, immunofluorescence showing increased nuclear localization of NFκB in *Msx1/Msx2*$^{d/d}$ uterus and pseudoimplantation sites (*Pseudo-IS*) under delayed conditions compared with control littermates after bortezomib treatment. *le*, luminal epithelium; *ge*, glandular epithelium; *s*, stroma. *Bars*, 250 μm.

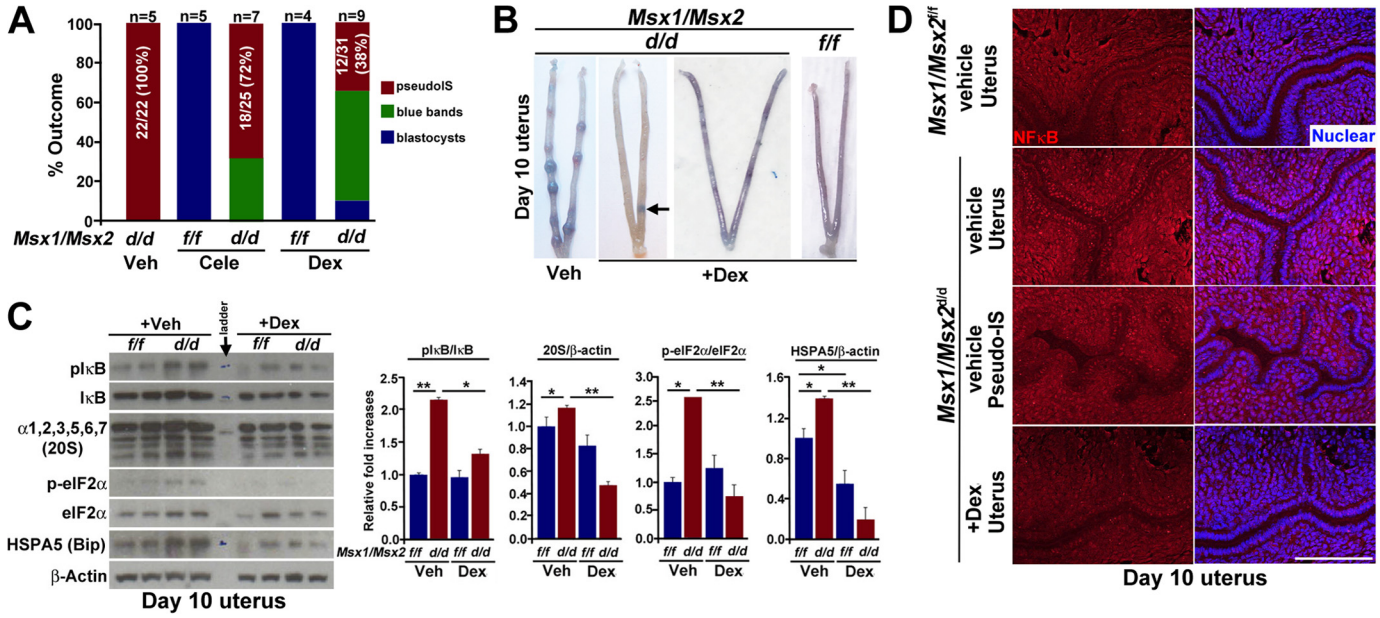

FIGURE 8. **Dexamethasone treatment reduces incidence of pseudoimplantation and NFκB-mediated inflammation in *Msx1/Msx2*$^{d/d}$ uteri under delayed conditions.** *A*, incidence of pseudoimplantation sites (*pseudoIS*) in vehicle- (*Veh*), celecoxib- (*Cele*), or dexamethasone-treated (*Dex*) *Msx1/Msx2*$^{d/d}$ uteri under delayed conditions. *Bars* showing color-coded segments represent the percentage of mice with pseudoIS (*red*), blue bands (*green*), and recovered blastocysts (*blue*). Although percentages of pseudoIS with faint or no blue bands at the site of blastocysts are shown within *parentheses* in the *red segments* of *bars*, numbers of mice used in each set of experiments are shown above the *bars*. *B*, representative images of *Msx1/Msx2*$^{d/d}$ uteri after vehicle or Dex treatment as compared with dexamethasone-treated floxed uteri. *Arrow*, faint blue band. *C*, *left panel*, Western blotting results showing reduced levels of pIκB, α-subunits of the 20S proteasome, p-eIF2α, and HSPA5/Bip in *Msx1/Msx2*$^{d/d}$ mice after dexamethasone treatment. *Right panels*, quantification of Western blotting results (means ± S.E.). *, $p < 0.05$; **, $p < 0.01$. *D*, immunofluorescence showing reduced nuclear NFκB expression in dexamethasone-treated *Msx1/Msx2*$^{d/d}$ uteri under delayed conditions. *Bar*, 250 μm.

Using proteomics and computational modeling, we identified dysregulation of several pathways in *Msx1/Msx2*$^{d/d}$ uteri with a signature of heightened inflammatory responses promoting a uterine environment unfavorable for embryonic diapause (7). Indeed, an inflammatory signature with increased phosphorylation of IκB, NFκB nuclear localization, and Cox2 induction was evident in *Msx1/Msx2*$^{d/d}$ uteri under delayed conditions. This is consistent with our findings of heightened proteasome activity facilitating enhanced destruction of targeted proteins, such as pIκB, by the proteasome. These findings suggest that Msx transcription factors play an important role in tempering inflammatory responses in the uterus.

The signature of enhanced inflammation and dysregulated proteasome activity seen in *Msx1/Msx2*$^{d/d}$ uteri are similar to that of pathological processes such as multiple myeloma, neurodegenerative diseases, non-Hodgkin's lymphoma, and autoimmune diseases (62–65). In addition, there is evidence that enhanced translation and accumulation of misfolded proteins incurs proteotoxic and ER stresses (10). These conditions engage chaperones and co-chaperones to direct refolding of misfolded proteins or targeting damaged proteins to the ubiquitin-proteasome machinery (45, 46, 52). Failure to relieve ER stress results in harmful cellular responses and apoptosis (42). Therefore, the ubiquitin-proteasome system maintains protein homeostasis for normal functioning, and its dysregulation in *Msx1/Msx2*$^{d/d}$ uteri suggests a role for Msx in protein homeostasis during embryonic diapause. It is interesting to note that ubiquitin pathway modifiers have been identified in diapausing cysts of the crustacean *Artemia sinica* (66) and *Caenorhabditis elegans* in dauer diapause (67), suggesting a role in protein turnover and homeostasis in various forms of diapause. Intriguingly, *Artemia* cysts has also been shown to up-regulate a diapause-specific protein chaperone (68).

We speculate that the up-regulation of proteasome subunits and activity served to limit proteotoxic burden from higher levels of misfolded proteins and attenuate unwarranted inflammation. This is consistent with our results of increased incidence of pseudoimplantation sites and evidence of ER stress (higher Bip levels) in the *Msx1/Msx2*$^{d/d}$ uteri after treatment with proteasome inhibitor bortezomib consistent with its reported mechanism of action (64). Our findings of enhanced NFκB nuclear localization and heightened ER stress in *Msx*-deleted uteri corroborate reports of enhanced NFκB-mediated inflammation and ER stress (69). In contrast, reduced incidence and size of pseudoimplantation sites in uteri under similar conditions after dexamethasone treatment suggests that unchecked inflammation in the absence of *Msx* is a major cause of failure of delayed implantation.

Msx deficiency is considered to enhance tumorigenesis in human breast cancer (70). Because inflammation is a hallmark of cancer progression, it is possible that dysregulation of Msx promotes the cancer phenotype via enhanced inflammatory signature in affected tissue types. In this regard, we believe that our study is the first to show the relationship between Msx activity and inflammation.

Proteins that incur antioxidant properties were also up-regulated in *Msx1/Msx2*$^{d/d}$ uteri under delayed conditions (supplemental Data Set S1, worksheets 4–6). Their up-regulation is perhaps an attempt to limit inflammation and promotion of anti-inflammatory mechanisms. However, we cannot

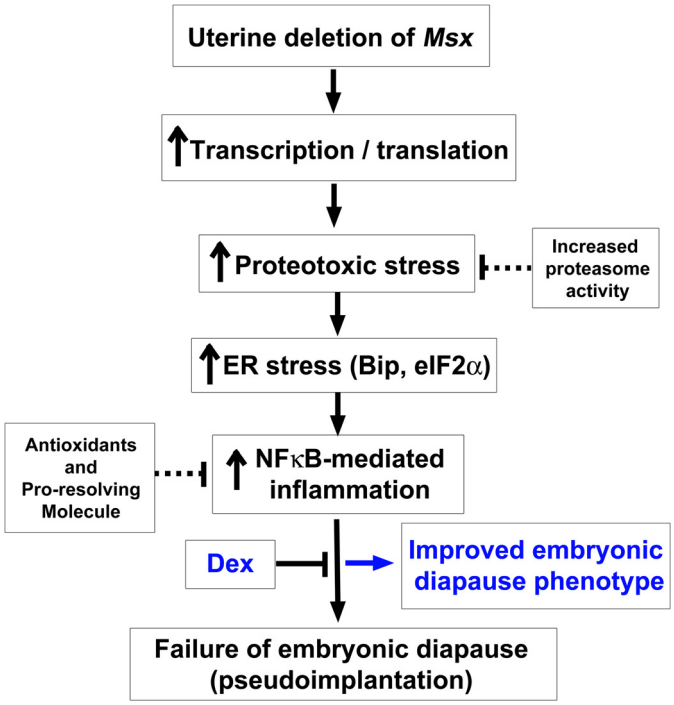

FIGURE 9. **A proposed scheme for the regulation of uterine inflammation for embryonic diapause by *Msx* genes.** Deletion of uterine *Msx* genes resulted in aberrant inflammation arising from increased transcription/translation, proteotoxic stress from protein burden, and ER stress. Inflammatory responses were reflected in higher NFκB signaling with premature termination of embryonic diapause and formation of pseudoimplantation sites caused by loss of synchrony between the blastocyst and uterus. Although proteasome components, antioxidants, and a pro-resolving molecule were up-regulated perhaps in an attempt to quell aberrant inflammation, these changes could not mitigate uterine inflammatory responses (*smaller font* and *dashed lines*). However, treatment with a long acting glucocorticoid dexamethasone (*Dex*) improved the embryonic diapause phenotype.

exclude the possibility that the up-regulation of unique antioxidants may have roles distinct from mitigating inflammation. Pro-resolving molecules are part of an active program to limit and resolve inflammation using the body's natural pathways (71). Interestingly, annexin A1, a pro-resolving molecule, was up-regulated in the uterus in the absence of Msx (supplemental Data Set S1, worksheets 4 – 6). This would suggest that the inflammatory responses dominated in *Msx*-deleted uteri and could not be quelled by antioxidants or pro-resolving molecules.

Furthermore, this study has identified other signaling hubs in the uterus that were altered in *Msx1/Msx2*$^{d/d}$ females incapable of undergoing delay. Msx transcription factors were previously shown to have roles in chromatin remodeling and transcriptional regulation and are considered to be global repressors with direct interaction with the Polycomb repressor complex (72, 73). This would suggest that deletion of *Msx* will lead to dysregulated transcriptional landscape in a biological system. Indeed, our proteomic results identified marked dysregulation in histones, chromatin remodeling, transcriptional regulatory components, and hnRNPs (supplemental Data Set S1, worksheets 4 – 6). Because our computational modeling and subsequent experimental analyses projected these changes toward enhanced inflammation, it is possible that alterations in these pathways also contributed to heightened inflammatory response. Whether the inflammatory signature imposed by inactivation by *Msx* are specific to the uterus or whether other tissues with inactivation of *Msx* also show a similar signature would require further investigation.

Collectively, this study points toward the magnitude and breadth of Msx function in the uterus and detrimental implications for pregnancy outcome in their absence. This mouse model has allowed us to investigate the scope and critical requirement of this homeotic protein family in uterine biology. The presence of this highly conserved transcription factor family in the uterus of other diapausing species such as the North American mink and Australian tammar wallaby during diapause underscores its substantial role in regulating uterine function across species (7).

This study also provides an opportunity to investigate the role of Msx and the candidate protein targets in embryonic diapause in mice and other species. Because the human endometrium also changes in the expression *MSX* genes during the menstrual cycle (28), these factors potentially have clinical implications in female fertility. This speculation is consistent with the observations of inflammation and reduced fertility in endometriosis and other pathological states of the endometrium. Thus, it would be intriguing to address the role of Msx in these diseases.

We believe that our model of aberrant inflammation in the uterus devoid of *Msx* genes would suggest that inflammation is tightly regulated during natural pregnancy and embryonic diapause (Fig. 9). Under normal conditions, exit from diapause induces blastocyst activation synchronized with uterine receptivity after implantation-inducing stimuli. This is in contrast to mice with uterine deletion of *Msx* genes that show poor embryo recovery and survival and formation of pseudoimplantation sites, which fail to produce a live birth. Taken together, these results propose a new concept that *Msx* genes have a major role in coordinating various pathways to limit inflammation in the mammalian uterus for embryonic diapause.

References

1. Cha, J., Sun, X., and Dey, S. K. (2012) Mechanisms of implantation: strategies for successful pregnancy. *Nat. Med.* **18,** 1754–1767
2. Ma, W. G., Song, H., Das, S. K., Paria, B. C., and Dey, S. K. (2003) Estrogen is a critical determinant that specifies the duration of the window of uterine receptivity for implantation. *Proc. Natl. Acad. Sci. U.S.A.* **100,** 2963–2968
3. Psychoyos, A. (1973) Endocrine control of egg implantation. in *Handbook of Physiology* (R. O. Greep, E. G. Astwood, and S. R. Geiger, eds) pp. 187–215, American Physiology Society, Washington, D. C.
4. Renfree, M. B., and Shaw, G. (2000) Diapause *Annu. Rev. Physiol.* **62,** 353–375
5. Lopes, F. L., Desmarais, J. A., and Murphy, B. D. (2004) Embryonic diapause and its regulation. *Reproduction* **128,** 669–678
6. Yoshinaga, K. (1961) Effect of local application of ovarian hormones on the delay in implantation in lactating rats. *J. Reprod. Fertil.* **2,** 35–41
7. Cha, J., Sun, X., Bartos, A., Fenelon, J., Lefèvre, P., Daikoku, T., Shaw, G., Maxson, R., Murphy, B. D., Renfree, M. B., and Dey, S. K. (2013) A new role for muscle segment homeobox genes in mammalian embryonic diapause. *Open Biol.* **3,** 130035
8. McLaren, A. (1968) A study of blastocysts during delay and subsequent implantation in lactating mice. *J. Endocrinol.* **42,** 453–463
9. Skaug, B., Jiang, X., and Chen, Z. J. (2009) The role of ubiquitin in NF-κB regulatory pathways. *Annu. Rev. Biochem.* **78,** 769–796
10. Wertz, I. E., and Dixit, V. M. (2010) Signaling to NF-κB: regulation by

ubiquitination. *Cold Spring Harb. Perspect. Biol.* **2,** a003350
11. Daikoku, T., Cha, J., Sun, X., Tranguch, S., Xie, H., Fujita, T., Hirota, Y., Lydon, J., DeMayo, F., Maxson, R., and Dey, S. K. (2011) Conditional deletion of Msx homeobox genes in the uterus inhibits blastocyst implantation by altering uterine receptivity. *Dev. Cell* **21,** 1014–1025
12. Baker, E. S., Clowers, B. H., Li, F., Tang, K., Tolmachev, A. V., Prior, D. C., Belov, M. E., and Smith, R. D. (2007) Ion mobility spectrometry-mass spectrometry performance using electrodynamic ion funnels and elevated drift gas pressures. *J. Am. Soc. Mass. Spectrom.* **18,** 1176–1187
13. Baker, E. S., Livesay, E. A., Orton, D. J., Moore, R. J., Danielson, W. F., 3rd, Prior, D. C., Ibrahim, Y. M., LaMarche, B. L., Mayampurath, A. M., Schepmoes, A. A., Hopkins, D. F., Tang, K., Smith, R. D., and Belov, M. E. (2010) An LC-IMS-MS platform providing increased dynamic range for high-throughput proteomic studies. *J. Proteome Res.* **9,** 997–1006
14. Livesay, E. A., Tang, K., Taylor, B. K., Buschbach, M. A., Hopkins, D. F., LaMarche, B. L., Zhao, R., Shen, Y., Orton, D. J., Moore, R. J., Kelly, R. T., Udseth, H. R., and Smith, R. D. (2008) Fully automated four-column capillary LC-MS system for maximizing throughput in proteomic analyses. *Anal. Chem.* **80,** 294–302
15. Zimmer, J. S., Monroe, M. E., Qian, W.-J., and Smith, R. D. (2006) Advances in proteomics data analysis and display using an accurate mass and time tag approach. *Mass Spectrom. Rev.* **25,** 450–482
16. Burnum, K. E., Hirota, Y., Baker, E. S., Yoshie, M., Ibrahim, Y. M., Monroe, M. E., Anderson, G. A., Smith, R. D., Daikoku, T., and Dey, S. K. (2012) Uterine deletion of Trp53 compromises antioxidant responses in the mouse decidua. *Endocrinology* **153,** 4568–4579
17. Kim, S., Gupta, N., and Pevzner, P. A. (2008) Spectral probabilities and generating functions of tandem mass spectra: a strike against decoy databases. *J. Proteome Res.* **7,** 3354–3363
18. Piehowski, P. D., Petyuk, V. A., Sandoval, J. D., Burnum, K. E., Kiebel, G. R., Monroe, M. E., Anderson, G. A., Camp, D. G., 2nd, and Smith, R. D. (2013) STEPS: A grid search methodology for optimized peptide identification filtering of MS/MS database search results. *Proteomics* **13,** 766–770
19. Jaitly, N., Mayampurath, A., Littlefield, K., Adkins, J. N., Anderson, G. A., and Smith, R. D. (2009) Decon2LS: An open-source software package for automated processing and visualization of high resolution mass spectrometry data. *BMC Bioinformatics* **10,** 87
20. Monroe, M. E., Tolić, N., Jaitly, N., Shaw, J. L., Adkins, J. N., and Smith, R. D. (2007) VIPER: an advanced software package to support high-throughput LC-MS peptide identification. *Bioinformatics* **23,** 2021–2023
21. Matzke, M. M., Waters, K. M., Metz, T. O., Jacobs, J. M., Sims, A. C., Baric, R. S., Pounds, J. G., and Webb-Robertson, B. J. (2011) Improved quality control processing of peptide-centric LC-MS proteomics data. *Bioinformatics* **27,** 2866–2872
22. Webb-Robertson, B. J., McCue, L. A., Waters, K. M., Matzke, M. M., Jacobs, J. M., Metz, T. O., Varnum, S. M., and Pounds, J. G. (2010) Combined statistical analyses of peptide intensities and peptide occurrences improves identification of significant peptides from MS-based proteomics data. *J. Proteome Res.* **9,** 5748–5756
23. Webb-Robertson, B. J., Matzke, M. M., Jacobs, J. M., Pounds, J. G., and Waters, K. M. (2011) A statistical selection strategy for normalization procedures in LC-MS proteomics experiments through dataset-dependent ranking of normalization scaling factors. *Proteomics* **11,** 4736–4741
24. Webb-Robertson, B. J., Matzke, M. M., Datta, S., Payne, S. H., Kang, J., Bramer, L. M., Nicora, C. D., Shukla, A. K., Metz, T. O., Rodland, K. D., Smith, R. D., Tardiff, M. F., McDermott, J. E., Pounds, J. G., and Waters, K. M. (2014) Bayesian proteoform modeling improves protein quantification of global proteomic measurements. *Mol. Cell. Proteomics* **13,** 3639–3646
25. Shannon, P., Markiel, A., Ozier, O., Baliga, N. S., Wang, J. T., Ramage, D., Amin, N., Schwikowski, B., and Ideker, T. (2003) Cytoscape: a software environment for integrated models of biomolecular interaction networks. *Genome Res.* **13,** 2498–2504
26. Hamazaki, J., Iemura, S., Natsume, T., Yashiroda, H., Tanaka, K., and Murata, S. (2006) A novel proteasome interacting protein recruits the deubiquitinating enzyme UCH37 to 26S proteasomes. *EMBO J.* **25,** 4524–4536
27. Kaneko, T., Hamazaki, J., Iemura, S., Sasaki, K., Furuyama, K., Natsume, T., Tanaka, K., and Murata, S. (2009) Assembly pathway of the mammalian proteasome base subcomplex is mediated by multiple specific chaperones. *Cell* **137,** 914–925
28. Wang, H., and Dey, S. K. (2006) Roadmap to embryo implantation: clues from mouse models. *Nat. Rev. Genet.* **7,** 185–199
29. Paria, B. C., Huet-Hudson, Y. M., and Dey, S. K. (1993) Blastocyst's state of activity determines the "window" of implantation in the receptive mouse uterus. *Proc. Natl. Acad. Sci. U.S.A.* **90,** 10159–10162
30. Chen, J., Bardes, E. E., Aronow, B. J., and Jegga, A. G. (2009) ToppGene Suite for gene list enrichment analysis and candidate gene prioritization. *Nucleic Acids Res.* **37,** W305–W311
31. Kaimal, V., Bardes, E. E., Tabar, S. C., Jegga, A. G., and Aronow, B. J. (2010) ToppCluster: a multiple gene list feature analyzer for comparative enrichment clustering and network-based dissection of biological systems. *Nucleic Acids Res.* **38,** W96–W102
32. Ahn, K. S., and Aggarwal, B. B. (2005) Transcription factor NF-κB: a sensor for smoke and stress signals. *Ann. N.Y. Acad. Sci.* **1056,** 218–233
33. Tegeder, I., Pfeilschifter, J., and Geisslinger, G. (2001) Cyclooxygenase-independent actions of cyclooxygenase inhibitors. *FASEB J.* **15,** 2057–2072
34. Yamamoto, Y., and Gaynor, R. B. (2001) Therapeutic potential of inhibition of the NF-κB pathway in the treatment of inflammation and cancer. *J. Clin. Invest.* **107,** 135–142
35. Dubois, R. N., Abramson, S. B., Crofford, L., Gupta, R. A., Simon, L. S., Van De Putte, L. B., and Lipsky, P. E. (1998) Cyclooxygenase in biology and disease. *FASEB J.* **12,** 1063–1073
36. Vane, J. R., and Botting, R. M. (1998) Anti-inflammatory drugs and their mechanism of action. *Inflamm. Res.* **47,** S78–S87
37. Glickman, M. H., and Ciechanover, A. (2002) The ubiquitin-proteasome proteolytic pathway: destruction for the sake of construction. *Physiol. Rev.* **82,** 373–428
38. Ravid, T., and Hochstrasser, M. (2008) Diversity of degradation signals in the ubiquitin-proteasome system. *Nat. Rev. Mol. Cell Biol.* **9,** 679–690
39. Schwartz, A. L., and Ciechanover, A. (2009) Targeting proteins for destruction by the ubiquitin system: implications for human pathobiology. *Annu. Rev. Pharmacol. Toxicol.* **49,** 73–96
40. Murata, S., Yashiroda, H., and Tanaka, K. (2009) Molecular mechanisms of proteasome assembly. *Nat. Rev. Mol. Cell Biol.* **10,** 104–115
41. Förster, F., Unverdorben, P., Sledź, P., and Baumeister, W. (2013) Unveiling the long-held secrets of the 26S proteasome. *Structure* **21,** 1551–1562
42. Sherman, M. Y. (2011) Proteotoxic stress targeted therapy (PSTT). *Oncotarget* **2,** 356–357
43. Weissman, A. M. (2001) Themes and variations on ubiquitylation. *Nat. Rev. Mol. Cell Biol.* **2,** 169–178
44. Husnjak, K., Elsasser, S., Zhang, N., Chen, X., Randles, L., Shi, Y., Hofmann, K., Walters, K. J., Finley, D., and Dikic, I. (2008) Proteasome subunit Rpn13 is a novel ubiquitin receptor. *Nature* **453,** 481–488
45. Sontag, E. M., Vonk, W. I., and Frydman, J. (2014) Sorting out the trash: the spatial nature of eukaryotic protein quality control. *Curr. Opin. Cell Biol.* **26,** 139–146
46. Clausen, T., Kaiser, M., Huber, R., and Ehrmann, M. (2011) HTRA proteases: regulated proteolysis in protein quality control. *Nat. Rev. Mol. Cell Biol.* **12,** 152–162
47. Esser, C., Alberti, S., and Höhfeld, J. (2004) Cooperation of molecular chaperones with the ubiquitin/proteasome system. *Biochim. Biophys. Acta* **1695,** 171–188
48. Barral, J. M., Broadley, S. A., Schaffar, G., and Hartl, F. U. (2004) Roles of molecular chaperones in protein misfolding diseases. *Semin. Cell. Dev. Biol.* **15,** 17–29
49. Kästle, M., and Grune, T. (2012) Interactions of the proteasomal system with chaperones: protein triage and protein quality control. *Prog. Mol. Biol. Transl. Sci.* **109,** 113–160
50. Tranguch, S., Cheung-Flynn, J., Daikoku, T., Prapapanich, V., Cox, M. B., Xie, H., Wang, H., Das, S. K., Smith, D. F., and Dey, S. K. (2005) Cochaperone immunophilin FKBP52 is critical to uterine receptivity for embryo implantation. *Proc. Natl. Acad. Sci. U.S.A.* **102,** 14326–14331
51. Tranguch, S., Wang, H., Daikoku, T., Xie, H., Smith, D. F., and Dey, S. K. (2007) FKBP52 deficiency-conferred uterine progesterone resistance is

genetic background and pregnancy stage specific. *J. Clin. Invest.* **117,** 1824–1834
52. Määttänen, P., Gehring, K., Bergeron, J. J., and Thomas, D. Y. (2010) Protein quality control in the ER: the recognition of misfolded proteins. *Semin. Cell. Dev. Biol.* **21,** 500–511
53. Das, S. K., Tan, J., Raja, S., Halder, J., Paria, B. C., and Dey, S. K. (2000) Estrogen targets genes involved in protein processing, calcium homeostasis, and Wnt signaling in the mouse uterus independent of estrogen receptor-α and -β. *J. Biol. Chem.* **275,** 28834–28842
54. Baker, E. S., Burnum-Johnson, K. E., Jacobs, J. M., Diamond, D. L., Brown, R. N., Ibrahim, Y. M., Orton, D. J., Piehowski, P. D., Purdy, D. E., Moore, R. J., Danielson, W. F., 3rd, Monroe, M. E., Crowell, K. L., Slysz, G. W., Gritsenko, M. A., Sandoval, J. D., Lamarche, B. L., Matzke, M. M., Webb-Robertson, B. J., Simons, B. C., McMahon, B. J., Bhattacharya, R., Perkins, J. D., Carithers, R. L., Jr., Strom, S., Self, S. G., Katze, M. G., Anderson, G. A., and Smith, R. D. (2014) Advancing the high throughput identification of liver fibrosis protein signatures using multiplexed ion mobility spectrometry. *Mol. Cell. Proteomics* **13,** 1119–1127
55. Oslowski, C. M., and Urano, F. (2011) Measuring ER stress and the unfolded protein response using mammalian tissue culture system. *Methods Enzymol.* **490,** 71–92
56. Kondratyev, M., Avezov, E., Shenkman, M., Groisman, B., and Lederkremer, G. Z. (2007) PERK-dependent compartmentalization of ERAD and unfolded protein response machineries during ER stress. *Exp. Cell Res.* **313,** 3395–3407
57. Kawabata, T., Tanimura, S., Asai, K., Kawasaki, R., Matsumaru, Y., and Kohno, M. (2012) Up-regulation of pro-apoptotic protein Bim and down-regulation of anti-apoptotic protein Mcl-1 cooperatively mediate enhanced tumor cell death induced by the combination of ERK kinase (MEK) inhibitor and microtubule inhibitor. *J. Biol. Chem.* **287,** 10289–10300
58. Ni, M., and Lee, A. S. (2007) ER chaperones in mammalian development and human diseases. *FEBS Lett.* **581,** 3641–3651
59. Johnson, D. C., and Dey, S. K. (1980) Role of histamine in implantation: dexamethasone inhibits estradiol-induced implantation in the rat. *Biol. Reprod.* **22,** 1136–1141
60. Bigsby, R. M., and Young, P. C. (1993) Progesterone and dexamethasone inhibition of uterine epithelial cell proliferation: studies with antiprogesterone compounds in the neonatal mouse. *J. Steroid Biochem. Mol. Biol.* **46,** 253–257
61. Daikoku, T., Song, H., Guo, Y., Riesewijk, A., Mosselman, S., Das, S. K., and Dey, S. K. (2004) Uterine Msx-1 and Wnt4 signaling becomes aberrant in mice with the loss of leukemia inhibitory factor or Hoxa-10: evidence for a novel cytokine-homeobox-Wnt signaling in implantation. *Mol. Endocrinol.* **18,** 1238–1250
62. Schwartz, A. L., and Ciechanover, A. (1999) The ubiquitin-proteasome pathway and pathogenesis of human diseases. *Annu. Rev. Med.* **50,** 57–74
63. McNaught, K. S., Olanow, C. W., Halliwell, B., Isacson, O., and Jenner, P. (2001) Failure of the ubiquitin-proteasome system in Parkinson's disease. *Nat. Rev. Neurosci.* **2,** 589–594
64. Adams, J. (2004) The development of proteasome inhibitors as anticancer drugs. *Cancer Cell* **5,** 417–421
65. Dawson, T. M., and Dawson, V. L. (2003) Molecular pathways of neurodegeneration in Parkinson's disease. *Science* **302,** 819–822
66. Yang, F., Jia, S. N., Yu, Y. Q., Ye, X., Liu, J., Qian, Y. Q., and Yang, W. J. (2012) Deubiquitinating enzyme BAP1 is involved in the formation and maintenance of the diapause embryos of *Artemia*. *Cell Stress Chaperones* **17,** 577–587
67. Horn, M., Geisen, C., Cermak, L., Becker, B., Nakamura, S., Klein, C., Pagano, M., and Antebi, A. (2014) DRE-1/FBXO11-dependent degradation of BLMP-1/BLIMP-1 governs *C. elegans* developmental timing and maturation. *Dev. Cell* **28,** 697–710
68. King, A. M., Toxopeus, J., and MacRae, T. H. (2014) Artemin, a diapause-specific chaperone, contributes to the stress tolerance of *Artemia franciscana* cysts and influences their release from females. *J. Exp. Biol.* **217,** 1719–1724
69. Kitamura, M. (2011) Control of NF-κB and inflammation by the unfolded protein response. *Int. Rev. Immunol.* **30,** 4–15
70. Lanigan, F., Gremel, G., Hughes, R., Brennan, D. J., Martin, F., Jirström, K., and Gallagher, W. M. (2010) Homeobox transcription factor muscle segment homeobox 2 (Msx2) correlates with good prognosis in breast cancer patients and induces apoptosis *in vitro*. *Breast Cancer Res.* **12,** R59
71. Serhan, C. N. (2014) Pro-resolving lipid mediators are leads for resolution physiology. *Nature* **510,** 92–101
72. Wang, J., Kumar, R. M., Biggs, V. J., Lee, H., Chen, Y., Kagey, M. H., Young, R. A., and Abate-Shen, C. (2011) The Msx1 homeoprotein recruits polycomb to the nuclear periphery during development. *Dev. Cell* **21,** 575–588
73. Wang, J., and Abate-Shen, C. (2012) The MSX1 homeoprotein recruits G9a methyltransferase to repressed target genes in myoblast cells. *PLoS One* **7,** e37647

Developmental Biology:

Muscle Segment Homeobox Genes Direct Embryonic Diapause by Limiting Inflammation in the Uterus

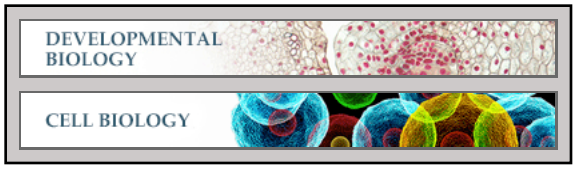

Jeeyeon Cha, Kristin E. Burnum-Johnson, Amanda Bartos, Yingju Li, Erin S. Baker, Susan C. Tilton, Bobbie-Jo M. Webb-Robertson, Paul D. Piehowski, Matthew E. Monroe, Anil G. Jegga, Shigeo Murata, Yasushi Hirota and Sudhansu K. Dey

J. Biol. Chem. 2015, 290:15337-15349.
doi: 10.1074/jbc.M115.655001 originally published online April 30, 2015
